JMB

The Funnel Approach to the Precrystallization Production of Membrane Proteins

Oded Lewinson, Allen T. Lee and Douglas C. Rees*

Division of Chemistry and Chemical Engineering 114-96, Howard Hughes Medical Institute, California Institute of Technology, Pasadena, CA 91125, USA

Challenges in the production of integral membrane proteins for structural studies include low expression levels, incorrect membrane insertion, aggregation and instability. In this report, we describe a "funnel approach" to overcoming these difficulties and demonstrate its efficacy in a case study of 36 prokaryotic P-type transporters. A diverse ensemble of modified constructs is generated and tested for expression in *Escherichia coli*, membrane localization, detergent extraction, and homogeneity. High-throughput methodologies are implemented throughout the process to facilitate identification of promising targets. We find that the choice of promoter, the choice of source organism providing the cloned gene, and, most importantly, the position of the affinity tag have a great effect on successful production. The latter had pronounced effects at all tested levels, from expression levels observed in whole cells to the extent of membrane insertion, and even on protein function. Following the initial streamlined screening, we were able to fine-tune and produce 9 of the 36 targets as materials suitable for crystallization or other structural studies.

Introduction

The passage of most biologically relevant molecules across the permeability barrier created by the cell membrane is mediated by specialized membrane proteins known as transporters. The significance of transport processes to cellular metabolism is emphasized by the observation that over 550 families of transporters have been identified through biochemical and genomic analyses†.[1] Despite recent successes and advances,[2] structural studies of transporters remain a formidable challenge. The relative paucity of structural information stands in clear contrast to the interest and importance of these proteins as pivotal participants in all physiological processes. Moreover, their membrane localization makes them attractive phar-

maceutical targets, and an increasing number of transporters have been directly implicated in human diseases.[3–8] An example of the physiological significance of membrane proteins may be provided by the P-type ATPases, a family of transporters characterized by unique signature motifs and functional and structural features.[9] Members of this family include the Na^+/K^+ ATPase, the gastric H^+ ATPase, and the sarcoplasmic reticulum (SR) Ca^{2+} ATPase. The hallmark of this family of pumps is the formation of a phosphoenzyme intermediate (hence the name P-type ATPase) by the transfer of the γ-phosphate from ATP to a conserved aspartic residue. Due to the pioneering efforts of Toyoshima and coworkers,[10,11] the SR Ca^{+2} ATPase has been solved in multiple conformations, and more recently, structures of the Na^+, K^+ and H^+ P-type ATPases have been reported by Nissen and coworkers.[12,13] These structures, representing various intermediates in the catalytic cycle, provide an explicit transport mechanism for this family of transporters.

Transition metal transporters that catalyze the extrusion of metals such as copper, zinc, lead, mercury, cadmium, manganese, and magnesium constitute a subclass of P-type ATPases loosely referred to as "heavy metal" or type P_{1B}.[14] While transition metals are crucial participants in many enzymatic reactions, intracellular concentrations of these me-

*Corresponding author. E-mail address:
dcrees@caltech.edu.
† http://www.tcdb.org
Abbreviations used: SR, sarcoplasmic reticulum; MCS, multiple cloning sites; LDAO, *N,N*-dimethyldodecylamine-*N*-oxide; OG, octyl-β-D-glucopyranoside; DDM, dodecyl-β-D-maltoside; $C_{12}E_8$, dodecyloctaoxyethylene; FC-14, Fos-choline 14; ORF, open reading frame.

tals are carefully controlled, since elevated levels are toxic. Transition metal P-type ATPases participate in this process by pumping cognate metals across the membrane; malfunctions of these proteins can lead to pathologies as manifested in Wilson disease and Menkes syndrome.[15] In view of their physiological functions, we have focused on this subgroup of transporters for structural analysis.

A variety of obstacles litter the path towards successful crystallization of a transporter or any other membrane protein. Not only do these proteins need to be overexpressed, correctly folded, and inserted into the plasma membrane *in vivo*, they also need to be subsequently extracted from it *in vitro*. Following extraction, the detergent-solubilized protein must be purified while retaining stability. To overcome these obstacles, we have developed a "funnel approach" based on the screening of multiple constructs to identify those suitable for structural studies.[16] This is the same strategy utilized by Kendrew and Parrish in the original structure determination of myoglobin,[17] except that rather than obtaining homologous proteins from different natural sources, one can now amplify the desired targets from genomic DNA. The basic idea is that if there is a 90% chance that a given protein will fail to crystallize, the probability that two different proteins will both fail is reduced to $0.9^2 = 81\%$ (i.e., success is more likely the more proteins that are tried). As practically implemented for prokaryotic transporters,[18] ~30 homologous genes of interest are chosen from a variety of host genomes. A diverse pool of constructs is generated from these genes, where each gene is represented by several slightly modified constructs. This pool of constructs is then subjected to a series of sequential tests aimed at judging their suitability for structural studies. Promising candidates proceed to the next stage, while the rest of the ensemble is discarded. The number of potential targets dwindles as more tests are applied, hence the funnel effect. The goal is to start with enough proteins so that one or more will survive to the end.

In the present work, we have amplified genes of 36 P-type ATPases from 11 different genomes and subcloned each gene into four different expression vectors (Table 1). The expression vectors harbor a polyhistidine affinity tag at either the N-terminus or the C-terminus position, and several constructs were also fused to an additional affinity tag. Further diversity is achieved by utilizing either the T7 or the arabinose promoter. An initial collection of 144 constructs was introduced into five different *Escherichia coli* strains, and expression in whole-cell lysates was evaluated using high-throughput techniques. Highly expressed proteins were then tested for membrane localization, followed by detergent-extraction screens. We found that the identity and location of the fused affinity tag have a significant effect at all stages, from expression levels observed in whole cells to membrane localization of the expressed proteins, detergent extraction, and protein

Table 1. List of genes described in this work

Organism	Accession number	Organism	Accession number
Escherichia coli	*P37617	*Streptococcus pneumoniae*	P35597
Escherichia coli	*NA[a]	*Thermoplasma volcanium*	Q978Z8
Escherichia coli	*P0ABB8	*Pseudomonas aeruginosa*	**Q9HXV0
Escherichia coli	*P03960	*Pseudomonas aeruginosa*	Q9HX93
Campylobacter jejuni	**Q9PNE0	*Pseudomonas aeruginosa*	*Q9I147
Campylobacter jejuni	Q9PND4	*Pseudomonas aeruginosa*	*Q9I3G8
Campylobacter jejuni	Q7AR91	*Pseudomonas aeruginosa*	**Q9HUY5
Pyrococcus furiosus	Q8TH11	*Archaeoglobus fulgidus*	**O29777
Helicobacter pylori	P55989	*Archaeoglobus fulgidus*	**O30085
Helicobacter pylori	O26033	*Ralstonia metallidurans*	**Q1LEH0
Helicobacter pylori	Q59465	*Ralstonia metallidurans*	*Q1LKZ4[b]
Rhizobium radiobacter	*Q8UH42	*Ralstonia metallidurans*	**Q1LKZ4[c]
Rhizobium radiobacter	**Q8UG47	*Ralstonia metallidurans*	*Q1LKZ4[d]
Rhizobium radiobacter	**Q8UGU8	*Ralstonia metallidurans*	*Q1LAJ7
Rhizobium radiobacter	*Q8UF71	*Proteus mirabilis*	*O33448
Streptococcus pneumoniae	Q97RR4	Human *Escherichia coli* chimera	*NA[e]
Streptococcus pneumoniae	Q97NE2	Human *Escherichia coli* chimera	*NA[f]
Streptococcus pneumoniae	*Q97PQ2	*Lactobacillus plantarum*	Q88VW3

Proteins that expressed well in the membrane fraction are denoted with an asterisk preceding the accession number. Proteins that expressed well and survived to the end of the funnel are preceded with an additional asterisk.

Within the phylum Proteobacteria, *E. coli*, *C. jejuni*, *H. pylori*, *Rh. radiobacter*, *P. aeruginosa*, *R. metallidurans*, and *Pr. mirabilis* are in the γ-, ε-, ε-, α-, γ-, β-, and α-proteobacteria classes, respectively. *S. pneumoniae* and *L. plantarum* belong to the phylum Firmicutes, while *Py. furiosus*, *T. volcanium*, and *A. fulgidus* belong to the domain Archaea, phylum Euryarchaeota.[20]

NA, not applicable.
[a] Δ-ZntA from Hou *et al.*[39]
[b] Alternative ORFs starting at the 1st amino acid.
[c] Alternative ORFs starting at the 51st amino acid.
[d] Alternative ORFs starting at the 103rd amino acid.
[e] Cu(6)-ZntA from Hou *et al.*[39]
[f] Cu(1–6)-ZntA from Hou *et al.*[39]

aggregation and stability, and even on protein function *in vivo*. N-terminal tagging is generally preferable to C-terminal tagging, and transcriptional control by the T7 promoter often results in an expression higher than that by the arabinose promoter. By using a combinatorial approach of multiple genes, constructs, and host strains, we were able to overproduce 24 out of 36 chosen targets. Twenty of these proteins were amenable to detergent extraction and were purified using single-step metal-affinity chromatography. Following purifications, candidate proteins were assayed for monodispersity and stability. By combining high-throughput methodology with standard biochemical methods, 25% (9 of 36) of the target proteins could be prepared in a purified, monodisperse, and stable form that is suitable for crystallographic trials.

Results

Amplification and molecular cloning of target genes

It has been our experience and those of others[21–23] that the expression level and properties of a given gene product are often affected by the type and position of the fused affinity tag. Accordingly, as detailed in Materials and Methods, we created a collection of constructs where each target gene is represented by several slightly modified clones. A custom multiple cloning site was engineered and inserted in place of the original multiple cloning sites (MCS) of pET19b, pET21d$^+$ (Novagen, San Diego, CA), pBAD/HisA, and pBAD Myc-His-C (Invitrogen, Carlsbad, CA). The modified vectors contained only the His-tag at either the N-terminal or the C-terminal position. All other fusions/additions originally present in these vectors were removed. Due to the identity of the MCS in all vectors, each target gene was amplified using only one set of oligonucleotides. Our final collection of clones consisted of 144 constructs representing different versions of 36 genes. In general (with a few exceptions), the following variants were constructed for each of the target genes: N-terminal His-tag, C-terminal His-tag, transcriptional control via the T7 promoter, and transcriptional control via the arabinose promoter. In several cases, a second affinity tag was also introduced.

Testing expression in whole cells

To simplify expression testing, plasmid DNA for the 144 clones was stored in 96-well plates. Similarly, chemically competent cells of the host strains were prepared in a 96-well-plate format. Standard transformation protocols were used, and transformed cells were plated onto a Luria–Bertani (LB) agar tray divided into a grid of 48 squares (Q-trays; Genetix USA). The optical densities of 150-μl cultures were continuously monitored in an automated plate reader (Saffire II; Tecan Austria), which facilitated

middle log-phase induction (Fig. 1a). The growth curves of the cultures harboring the different pBAD (arabinose promoter) constructs were more uniform relative to those harboring the pET (T7 promoter) constructs (compare Fig. 1a, left and right panels, respectively). Postinduction, the pBAD constructs generally continued to grow normally, while the growth of many of the pET constructs stopped, with some cultures lysing. The initial expression studies for all clones utilized *E. coli* strain BL21(DE3) GOLD™ (Stratagene). Expression was tested at three different temperatures (37 °C, 28 °C, and 23 °C), along with variations in the duration of induction times and inducer concentrations (see Materials and Methods for details). To semiquantitatively assess the results, expression levels were categorized relative to the expression level of the vitamin B12 transporter BtuCD that was previously found to express and purify well.[18] The His-tagged protein content of each culture well was analyzed using dot-blot techniques (Fig. 1b). Sixty-two of the 144 clones showed expression levels equal to or higher than that of BtuCD and were defined as high-
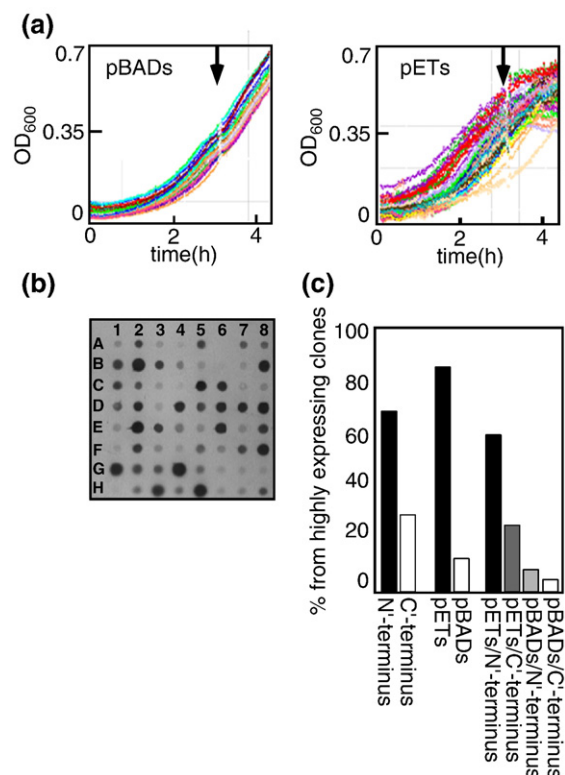

Fig. 1. Expression in whole-cell lysates. (a) Growth in an automated plate reader of *E. coli* BL21(DE3) GOLD™ expressing 48 different pBAD constructs (left panel) and 48 different pET constructs (right panel). Arrows indicate the time of induction. (b) Dot-blot analysis of whole-cell lysates of 64 pBAD constructs. Wells C6 and C7: open reading frame (ORF) Q9HXV0 His-tagged at the N-terminus or the C-terminus, respectively. Wells F6 and F7: Cu (1–6)–ZntA His-tagged or Myc-His-tagged, respectively. (c) Distribution of highly expressing clones according to tag position and vector type.

level expressors; 29 clones showed expression levels twofold to threefold lower than that of BtuCD (i.e., medium level); and 52 clones had very low expression levels (i.e., low level).

The most evident observation that emerges from this set of experiments is the significant influence of the affinity-tag location. In many instances, an N-terminal His-tagged protein expresses well, while the same protein tagged at its C-terminal did not (Fig. 1b, compare well C6 to well C7). The opposite situation was also observed, although at a lower frequency (Fig. 1c). More striking are incidents where the presence of a second tag, adjacent to the His-tag, changes the expression level of a given protein (Fig. 1b, compare well F6 to well F7). The choice of promoter is also important, as the T7 promoter typically resulted in an expression higher than that with the arabinose promoter, although, again, there are exceptions (Fig. 1c). Another factor that influences expression levels is the temperature of induction. In 138 clones out of the tested 144 (∼96%), the best results were obtained when inducing for 2–3 h at 28 °C.

We next explored whether we could improve expression by using different *E. coli* strains. All constructs that expressed poorly in the BL21(DE3) GOLD™ strain were introduced into four additional strains: BL21(DE3) RIPL™, BL21(DE3) Star™, BL21 (DE3) C41/pLysS, and BL21(DE3) C43/pLysS. The BL21(DE3) RIPL™ strain carries a plasmid encoding tRNA for codons rarely used in *E. coli*; however, none of the constructs tested in this strain showed elevated expression. Sixteen percent of tested clones showed a somewhat elevated expression with the BL21(DE3) C41 pLysS and BL21(DE3) C43 pLysS strains that were selected for enhanced membrane protein expression.[24] The biggest improvement was observed with the BL21(DE3) Star™ strain containing a mutation in the *rne131* gene. This strain is characterized by greater mRNA stability and, indeed, 60% of the tested clones showed increased levels of expression. Overall, by using this combination of constructs and host strains, we were able to overexpress 82 constructs, representing 35 of the 36 target genes.

Membrane localization of the expressed proteins

While overexpressed membrane proteins can successfully integrate into the plasma membrane,[25–27] in other cases, they may not correctly incorporate into the plasma membrane and instead form insoluble aggregates or inclusion bodies.[28,29] Despite the time-consuming nature of membrane-fraction preparations, we wished to examine the correlation between expression levels observed in the whole-cell lysates and expression levels observed in the membrane. We thus prepared membrane vesicles from 63 of our highest expressing clones, representing 35 different genes. Surprisingly, only 29 of the 63 (46%) constructs found to express at high levels in whole-cell lysates also highly expressed in the membrane fraction (again, relative to the corresponding levels

of BtuCD). Eight of these 63 (13%) were present at low levels, despite their high presence in the whole-cell lysates. Twenty-six of the 63 (41%) were completely absent from the membrane fraction and were only found in the pellet of low-speed centrifugation following cell disruption, suggesting that they were present as inclusion bodies or aggregates. Seven of the 34 clones (20%) that localized poorly to the membrane of the BL21(DE3) GOLD™ strain could be expressed at higher levels in the BL21(DE3) Star™ strain. Overall, 36 constructs representing 24 different genes were found to express in the membrane at levels higher than or equal to the expression level of BtuCD (Table 1).

As observed in lysates of whole cells, the type and the position of the affinity tag can also influence the extent of membrane incorporation. When examining pairs of constructs of the same gene that showed similar expression levels in the whole-cell lysates, several cases were observed to have pronounced differences in membrane-fraction content (Fig. 2a). Differences were manifested not only in expression levels but also by the presence of additional bands in SDS-PAGE analysis. These bands, often of smaller size, presumably represent products of degradation or products of incomplete translation. We also noted that, in several of the examined pairs, a second affinity tag (adjacent to the His-tag) resulted in alteration of the extent of membrane incorporation and in the appearance of additional bands (Fig. 2a). As with whole-cell expression, N-terminal tagging also proved advantageous with respect to levels of membrane expression, since 64% of the clones that were highly expressed in the membrane were tagged at their N-terminus (Fig. 2b).

At the whole-cell level, transcription regulation by the T7 promoter resulted in expression levels higher than those achieved by the arabinose promoter (Fig. 1c). This difference was less pronounced in membranes, however, as 40% of the highly expressing proteins in this case were expressed as pBAD constructs, relative to only 13% at the whole-cell level (compare Fig. 1c to Fig. 2b). In general, the correlation between expression levels in whole cells and expression levels in the membrane was better for the pBAD constructs than for the pET constructs. Figure 2c shows a semiquantitative analysis (see Materials and Methods for details) of this effect for a subset of 24 pBAD constructs and 24 pET constructs representing a wide range of expression levels (0.75–6.8 μg/ml for the pBAD constructs and 2.6–17.2 μg/ml for the pET constructs). The correlation between whole-cell expression and membrane expression for the pBAD constructs is essentially linear over the whole expression range. In contrast, the correlation between whole-cell expression and membrane expression is much less evident for the pET constructs (Fig. 2c, right panel, solid line). Interestingly, for the subset of pET constructs expressing at lower levels (in the range of 2.6–8 μg/ml), a linear fit is clearly evident (Fig. 2c, right panel, dashed line) and similar to the fit of the complete set of pBAD constructs.
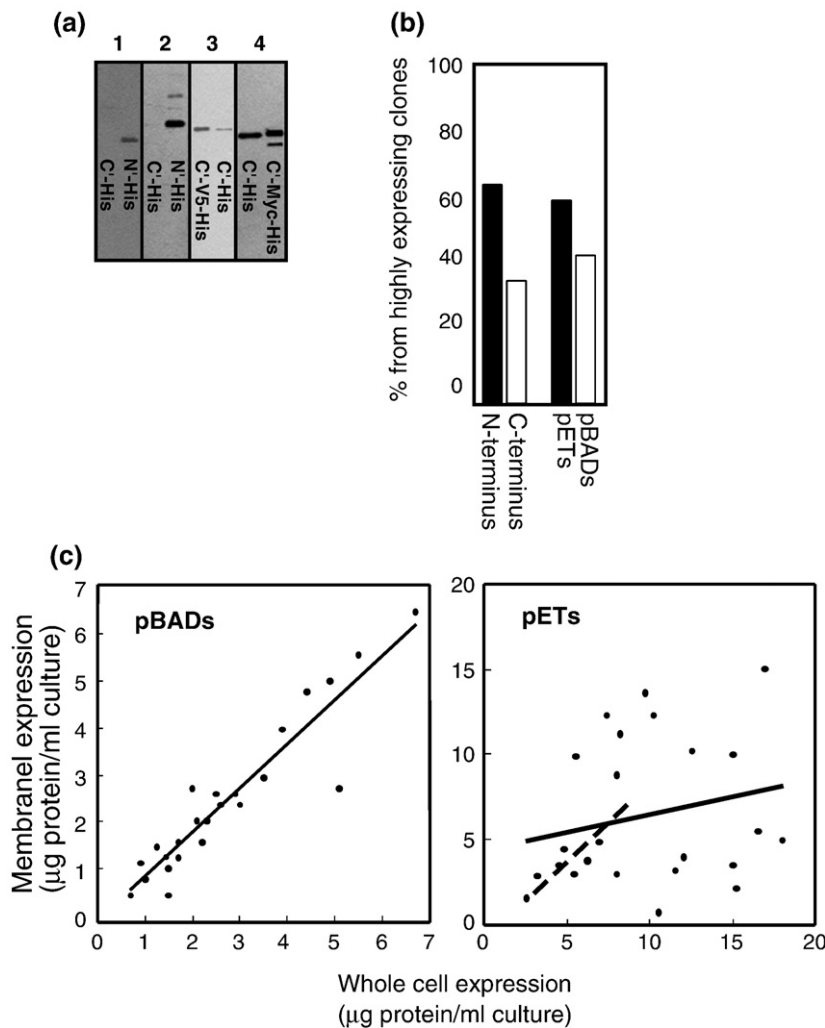
Fig. 2. Membrane-associated expression. (a) Western blot analysis of His-tagged protein expression in the membrane fraction. Lane 1, C-terminal and N-terminal His-tagged versions of ORF O29777. Lane 2, C-terminal and N-terminal His-tagged versions of ORF Q1LKZ4. Lane 3, C-V5-His and C-His-tagged versions of ORF Q9PNE0. Lane 4, C-terminal His and C-terminal Myc-His-tagged versions of Cu(6)-ZntA. (b) Distribution of highly expressed membrane-fraction constructs according to tag position and vector type. (c) Correlation between expression levels observed in whole cells and those observed in the membrane fraction. Left panel: pBAD constructs; right panel: pET constructs. In both panels, each point is an individual protein, and the linear fit is depicted as a solid line. In the right panel only, the dashed line represents the linear fit when only data up to 8 μg protein/ml culture are included.

Detergent extraction of membrane proteins

An essential step in crystallographic studies of membrane proteins is their detergent-mediated extraction from the membrane. The choice of detergent is crucial, since it has significant implications for protein oligomeric state, integrity, and function. Changes in head group size, chemical nature, and chain length can result in inactivation of the target protein, a highly undesirable consequence.[30–32] Moreover, detergent molecules may also effect crystal formation, and often a membrane protein that will crystallize in one detergent will not crystallize in another. Of the plethora of commercially available detergents, we opted to test only the following four: N,N-dimethyldodecylamine-N-oxide (LDAO), octyl-β-D-glucopyranoside (OG), dodecyl-β-D-maltoside (DDM), and dodecyloctaoxyethylene ($C_{12}E_8$). These detergents have been successfully used in the past in functional and crystallographic studies of numerous membrane proteins‡; furthermore, $C_{12}E_8$ was used in

the crystallization of rabbit SR Ca^{2+} ATPase.[10] Membrane preparations of each protein were placed on a 96-well plate, and the test detergent was added directly to the wells. Following agitation, soluble and insoluble fractions were separated by brief ultracentrifugation. Figure 3a shows the results of such an extraction assay. Twenty-nine of the 36 constructs (representing 20 genes) could be extracted in soluble form with at least one of the test detergents, and often with more than one. The most efficient detergent was DDM, closely followed by LDAO. Overall, OG resulted in lower extraction levels than with either DDM or LDAO, while the least efficient detergent for extraction was $C_{12}E_8$. When the membranes were treated with the more aggressive detergent Foscholine 14 (FC-14), much higher extraction levels were observed. In some instances, proteins that could not be extracted at all with the four "mild" detergents were efficiently extracted by FC-14 (Fig. 3b).

Purification and stability of the chosen targets

We next proceeded to purify 20 proteins that showed adequate levels of membrane-associated expression and could be extracted with at least one of the mild detergents. Most of these proteins (17 of

‡For a comprehensive list, see http://blanco.biomol. uci.edu/Membrane_Proteins_xtal.html, http://www. mpdb.ul.ie, and http://www.mpibp-frankfurt.mpg.de/ michel/public/memprotstruct.html
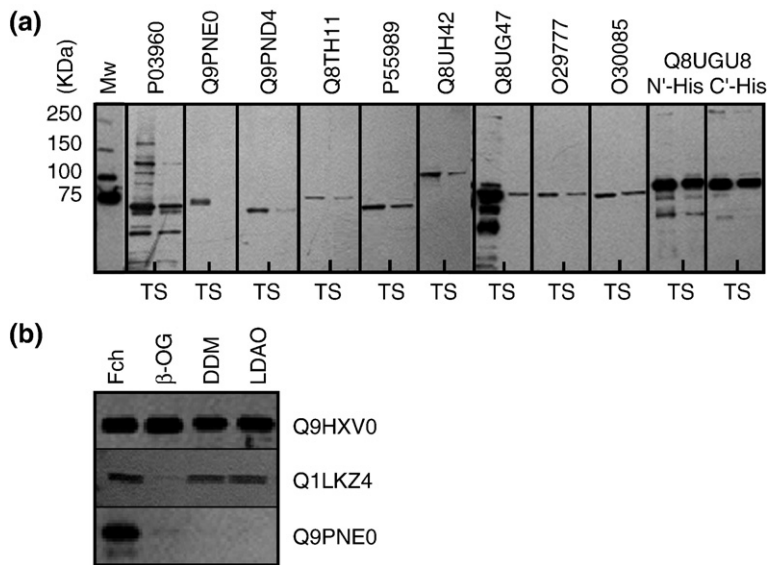
Fig. 3. Western blot analysis of detergent-extraction assays. (a) Membrane vesicles of 11 different proteins (accession numbers given on top of each panel) were incubated with 1% DDM. T, total membrane-fraction content; S, soluble fraction following detergent extraction. (b) Soluble fractions following detergent extraction of ORFs Q9HXV0, Q1LKZ4, and Q9PNE0, as indicated. One percent of either FC-14, OG, DDM, or LDAO was used.

20) could be purified to 80–90% homogeneity using single-step metal-affinity chromatography. Figure 4 shows an ensemble of such purifications representing different levels of purity and yield. In general, yields varied between 0.5 and 2 mg of pure protein per liter of culture. Since our goal at this stage of the process is the initial identification of promising targets, we did not attempt to further refine these crude purifica-

Fig. 4. Coomassie-blue-stained SDS gel electrophoresis analysis of protein purification through Ni-NTA affinity chromatography. Six purifications are shown, with accession numbers indicated adjacent to each panel. Lane 1, total membrane protein. Lane 2, soluble fraction following detergent extraction. Lane 3, unbound material. Lane 4, wash with 60 mM imidazole. Lane 5, wash with 100 mM imidazole. Lane 6, wash with 200 mM imidazole. Lane 7 (where applicable), wash with 350 mM imidazole.

tions. Rather, we proceeded to examine the monodispersity and stability of the selected targets. For this purpose, each of the purified proteins was concentrated to 10–20 mg/ml and injected onto a gel-filtration column (Superdex 200; GE Healthcare). These concentrated protein preparations were stored either at 4 °C or at room temperature, or snap-frozen in liquid nitrogen and stored at −80 °C. Following 7–10 days of storage at the different temperatures, the protein samples were reanalyzed by gel-filtration chromatography. Figure 5 shows the elution profiles of several proteins, both at the time of preparation and following storage. While certain proteins displayed an elution profile that was independent of storage length or temperatures, others that initially exhibited a high level of monodispersity developed additional peaks corresponding to higher-molecular-weight species upon storage. In some of the latter cases, a high-molecular-weight peak eluting in the void volume of the column (representing protein aggregation) could be removed by ultracentrifugation (Fig. 5b). Monodispersity is often affected by the type of detergent used for extraction, and this choice may need to be reevaluated at this stage (Fig. 5c). Of the 17 proteins subjected to this analysis, nine were found to retain monodispersity under all tested conditions and were consequently categorized as suitable targets for crystallization trials.
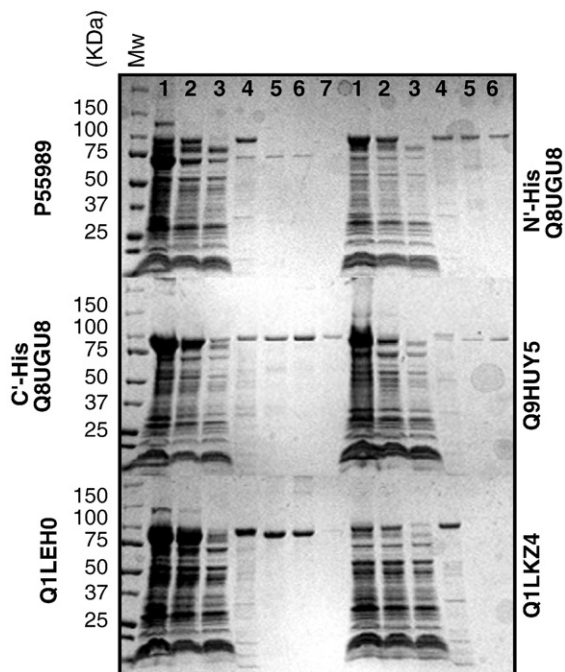
Discussion

In recent years, two general approaches for the structural analysis of membrane proteins have emerged. The first approach capitalizes on intimate knowledge of a specific protein of interest that often derives from years of comprehensive research. Functional, structural, and genetic data are combined to find conditions that will allow crystallization of a single specific membrane protein. Notable examples of membrane-embedded transporters whose structures have been so determined are the lactose
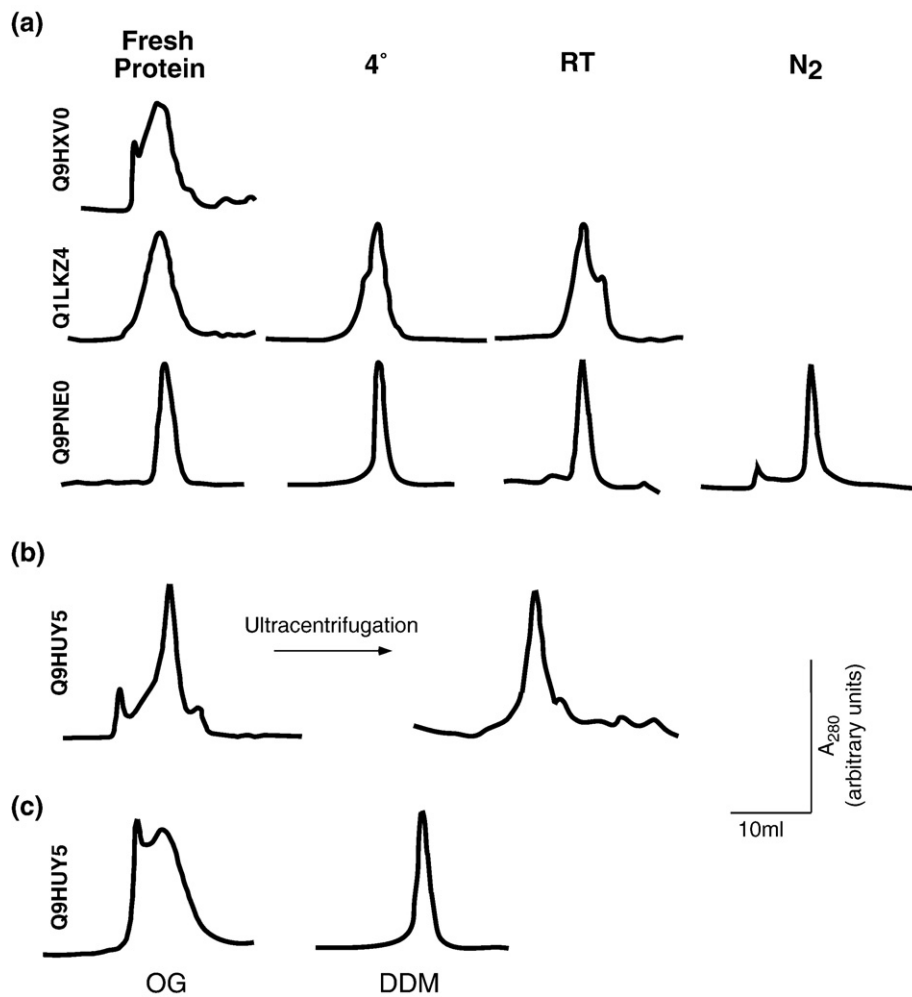
Fig. 5. Elution profiles following size exclusion chromatography of different protein preparations, with accession numbers indicated adjacent to each panel. (a) Profiles at the time of preparation (fresh protein) or following 10-day storage at either 4 °C, room temperature (RT), or liquid nitrogen (N_2). (b) Elution profile of ORF Q9HUY5 before or after ultracentrifugation. (c) Elution profiles of ORF Q9HUY5 when either DDM or OG was used for extraction.

permease[33] and the sodium/proton transporter NhaA[34] from *E. coli*. In contrast, the second approach targets a related family of proteins, rather than a specific protein, taking advantage of the large number of homologues that have been identified through genomic sequencing studies to identify particular proteins amenable to structural study. This funnel approach to membrane protein structure was employed, for example, in our structural analysis of the mechanosensitive channel of large conductance.[16]

The fundamental bases of the funnel approach are diversity and selection. For prokaryotic targets, 30–40 homologues are typically cloned and inserted into multiple expression vectors. This pool of constructs is then tested for expression in several *E. coli* strains. As expression levels observed in whole cells do not necessarily correspond to expression in the membrane fraction, the second stage of our screen is the testing of highly expressing clones for membrane localization of the protein targets. Once membrane-fraction localization is confirmed, several mild deter-

gents are assayed for their extraction ability. Metal-affinity chromatography is then used for initial purification, and the monodispersity of the purified proteins is evaluated using gel-filtration chromatography. Proteins exhibiting a high level of mono-dispersity are then reexamined following storage at different temperatures. Only those proteins that express at adequate levels in the membrane fraction, that can be extracted using a mild detergent, that can be purified to near homogeneity, and that can display monodispersity over time are considered promising targets for crystallization trials.

In the present report, we describe the feasibility of and analyze the various stages of the funnel approach as exemplified in a study of 36 metal P-type transporters.

Target selection

Our initial selection of targets was based primarily on the availability of genetic material. Nevertheless, a closer look at the results suggests that a more

rational choice at the initial stage of such a project may lead to higher success rates. In the study described here, proteins found to express well in the membrane fraction were clustered according to their taxonomy. Membrane-associated expression was highest (see Table 1) for proteins from organisms belonging to the same phylum as *E. coli*, the Proteobacteria. Even within this phylum, notable differences between classes were apparent. In addition to the three *E. coli* proteins, almost all of α, β, or γ subdivision proteins expressed at high levels (13 out of 14 tested). In contrast, only 1 of the 6 tested ε-subdivision proteins expressed well. Success rates were also low (1 out of 4) for *Streptococcus pneumoniae* proteins, a bacterium that belongs to a different phylum (Firmicutes) and is thus further removed from *E. coli*. Due to the relatively low number of subjects, the statistical significance of these observations is questionable. (This is also true for archaeal genes, where only one to two genes from a given organism were tested.) However, it seems that successful expression may be influenced by the taxonomic proximity between the host organism and the source organism. This proposal may be supported, in part, by the observation that a substantial majority of polytopic α-helical membrane proteins whose structures have been solved to date have been produced from their native tissues. No structure of an ε-subdivision membrane protein has been solved, despite the considerable attention that *Helicobacter pylori* has received in recent years. In comparison, several structures of membrane proteins derived from γ-proteobacteria, including those of transporters, have been reported. In all these cases, the proteins have been produced in *E. coli*.[35] In this regard, it is interesting to note that the membrane compositions of *E. coli* and other γ-proteobacteria are similar to each other, yet very different from those of ε-subdivision bacteria (*Campylobacter jejuni* and *H. pylori*).[19,36–38] Clearly, more detailed studies are necessary in order to establish such a connection, but the hypothesis that genetic proximity and/or compatible membrane compositions may effect successful heterologous expression is appealing.

Choice of promoter

Each of the tested proteins was expressed under the control of the T7 or the arabinose promoter. When expression level was estimated by analyzing the protein content of whole-cell lysates, the T7 promoter appeared to be greatly advantageous (Fig. 1c). However, when expression level was estimated by analyzing protein content in the membrane fraction, this apparent advantage was greatly diminished (Fig. 2b). The correlation between the expression level observed in whole-cell lysates and the expression level observed in the membrane fraction was better for proteins expressed under the control of the arabinose promoter (Fig. 2c). The observation that proteins expressed under the control of the T7 promoter more often resulted in

insoluble aggregates may be due, in part, to very high levels of expression that exceed the capacity of the membrane. It may also be that the rate of translation exceeds the maximal rate of insertion. To partially solve the problem of membrane incorporation, one may try to slow the rate of translation. This can be achieved by either lowering the temperature (postinduction) or varying the concentration of the inducer. In our hands, almost without exception, improved membrane integration was achieved this way without compromising total yields.

Effects of the affinity-tag position

The location and the identity of the affinity tag had a dramatic effect on expression levels (Fig. 1) and on the extent of membrane insertion (Fig. 2). Generally, N-terminal tagging resulted in higher levels of membrane-inserted protein. Nevertheless, for about one-third of the proteins, C-terminal tagging was preferable. The magnitude of the "tag effect" was quite surprising, sometimes altering expression by 100-fold (Figs. 1 and 2). Due to the extent of these effects, and since the goal of X-ray crystallography is to provide information on correctly folded and functionally relevant proteins, we extended our investigation of the "tag effect" to functional studies. Activity as a function of tag position was determined for four proteins using *in vivo* metal resistance assays.[39] Essentially, the proteins were tested for their ability to rescue the growth of *E. coli* GG48, a Zn^{2+}/Cd^{2+}-sensitive strain.[40] In three out of the four test cases, significant differences between the activities of the N-terminus and the C-terminus versions were observed (Fig. 6a–c). For example, at 60 μM $ZnCl_2$, the C-terminus version of *Ralstonia metallidurans* ZntA did not support growth any better than the empty vector, while the growth of cells expressing the N-terminus version was inhibited only by 40% (Fig. 6a). The opposite was true for *R. metallidurans* CadA (Fig. 6b), where the C-terminus version performed better. The most obvious differences were observed in the case of Cu(6)-ZntA, the human *E. coli* chimera (Table 1). Regardless of metal concentration, the C-terminus version conferred no growth advantage relative to the empty vector, whereas cells expressing the N-terminus version grew substantially better (Fig. 6c). Only in the case of *E. coli* ZntA did the growth phenotypes seem independent of the position of the tag (Fig. 6d). The observed differences could not be attributed to differences in expression levels, since with both *R. metallidurans* CadA and Cu(6)-ZntA, the more active form was the one that expressed to a lesser extent. For many transport proteins, simple growth rescue experiments can be performed at the early stages of the screening process. For importers, that assay may be based on growth rescue under conditions of a limiting concentration of a relevant metabolite. For exporters, increasing concentrations of a toxic compound can be used, as was shown here and extensively performed with multidrug transporters. The simplicity of these assays, com-
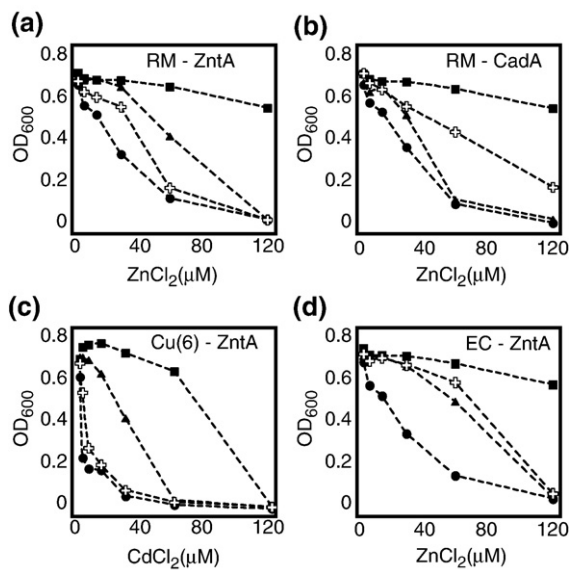
Fig. 6. Metal sensitivity growth experiments. *E. coli* W3110 (wild-type strain, insensitive to metals) or *E. coli* GG48 (mutant strain, sensitive to Cd^{2+} and Zn^{2+}) was cultured in the presence of the indicated metal concentrations. In all panels: squares: W3110/pBAD N (empty vector); circles: GG48/pBAD N (empty vector); triangles: GG48 cells expressing the N-terminal-tagged version of the indicated protein; crosses: GG48 cells expressing the C-terminal-tagged version of the indicated protein. (a) *R. metallidurans* ZntA. (b) *R. metallidurans* CadA. (c) Human *E. coli* chimera Cu(6)-ZntA. (d) *E. coli* ZntA.

bined with the abundance of *E. coli* deletion strains that can be used as hosts, makes these approaches readily accessible. Early identification of the active/inactive form of the target protein may save much labor and time. In retrospect, our efforts aimed at the large-scale production, purification, and stabilization of the C-terminus version of *R. metallidurans* ZntA (Fig. 4) probably would have been better directed towards the N-terminus-tagged version of the same protein.

A recent study by Rapp *et al.* demonstrated the effect of point mutations of charged residues on membrane protein topology and membrane insertion.[41] In light of these findings, it is not surprising that addition of multiple positively charged imidazoles at either the N-termini or the C-termini could have profound effects on overall expression, membrane incorporation, and even function.

Choice of detergent

Once membrane integration of the target proteins is established, a suitable detergent must be identified for membrane extraction. In the absence of prior functional or structural knowledge of the protein, a good starting point is to employ detergents used previously in structural studies. Three detergents stand out with respect to successful crystallization of polytopic inner membrane proteins: LDAO, OG, and DDM; $C_{12}E_8$ was also tested, since it was used in the

crystallization of the Ca^+ ATPase. With these four detergents, 20 of the 24 membrane proteins (29 of 36 constructs) could be extracted from the membrane, with DDM displaying the highest efficiency. When mild detergents fail, more aggressive ones may be more effective. Treatment with FC-14 resulted in much higher levels of extracted protein, and almost all of the tested proteins could be extracted using this detergent (Fig. 3). For reasons mentioned above, however, caution should be exercised when using harsh detergents. FC-14, for example, has been reported to be used in the structural analysis of only one protein, MscS,[42] and it is likely that the structure may not correspond to the closed resting state present in the membrane.[43]

A summary of the various stages of the funnel approach presented in this work is depicted in Fig. 7. Starting with 144 constructs (representing 36 genes), expression is first tested in whole cells. Each of the constructs was introduced into five different *E. coli* strains and tested for expression at different temperatures. Despite the large number of combinations (~2000), this step is quite brief, as high-throughput methodology allows for rapid identification of promising candidates.[44] This relatively rapid stage allowed us to identify favorable conditions for the expression of 82 constructs and to eliminate poorly expressing constructs from further consideration. As a next step, membrane fractions were prepared, and membrane-associated expression was evaluated. Thirty-six constructs (representing 24 genes) proved to be adequately incorporated into the plasma membrane and were tested in detergent-extraction assays. Twenty-nine of these constructs (representing 20 genes) were sufficiently extracted using mild detergents, while the complete set could be extracted using harsher ones. A subset of 20 constructs, representing 20 genes, was subsequently purified using single-step metal chromatography. Seventeen of these were purified to 80–90%, with yields of 0.5–
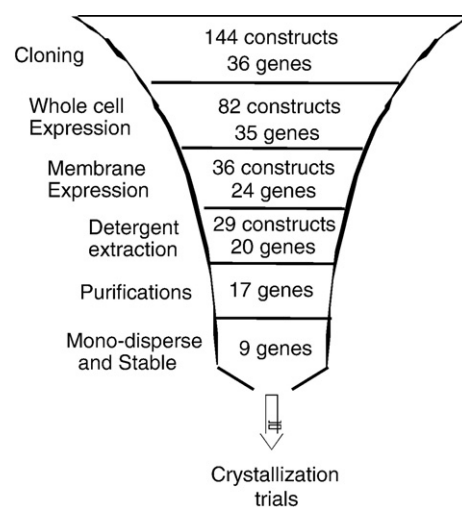

Fig. 7. Summary of the funnel approach presented in this work, with the number of gene products remaining at each stage indicated.

2 mg of pure protein per liter of culture. Of these 17 proteins, 9 displayed the desirable single-peak appearance when analyzed by gel-filtration chromatography and maintained the same appearance over time (Table 1). The overall yield reported here (9 of 36; 25%), combined with the increasing number of potential targets identified through genomic sequencing, provides a basis for some optimism that the structural characterization of prokaryotic membrane proteins is a tractable objective.

Materials and Methods

Unless otherwise stated, all chemicals were purchased from Sigma, and detergents were purchased from Anatrace.

Bacterial strains and molecular cloning techniques

E. coli strains BL21(DE3) GOLD™ and BL21(DE3) RIPL™ were obtained from Stratagene. Strain BL21(DE3) Star™ was obtained from Invitrogen, and strains BL21 (DE3) C41/pLysS and BL21(DE3) C43/pLysS were purchased from Lucigen Corporation. Restriction enzymes were obtained from Roche Diagnostics, and DNA polymerase was purchased from Finnzymes. The sequences of oligonucleotides used for amplification of target genes are available upon request. The original MCS of pET19b, pET21d⁺ (Novagen), pBAD/HisA, and pBAD Myc-His-C (Invitrogen) were replaced with GAATTCGGTACCG-TACGCTCGAGCTCTTCGAA.

Plasmid DNA was stored in a 96-well format, as were chemically competent cells of the host strains. Standard protocols were used to perform transformations in the 96-well format.

Expression testing in whole cells

Single colonies were used to inoculate 150 µl of LB medium in 96-well plates. To avoid precipitation, overnight cultures were grown at 30 °C under vigorous agitation (300 rpm). Cultures were then diluted 50-fold into 150 µl of Terrific broth media and grown in an automated plate reader (Saffire II; Tecan Austria). Cell growth was conducted at a temperature of 23 °C, 28 °C, or 37 °C. Depending on the growth temperature, expression was induced as follows: 23 °C: 0.1 mM IPTG or 0.02% L-arabinose for 16 h; 28 °C: 0.1 mM IPTG or 0.02% L-arabinose for 2–3 h; 37 °C: 1 mM IPTG or 0.2% L-arabinose for 1 h. To evaluate expression, 10 µl from each culture well was added to 200 µl of 20 mM Tris–HCl, 150 mM NaCl, and 1% SDS (pH 7.5) in a deep-well block. This block was then sealed with adhesive aluminum tape and heated to 95 °C for 10 min. Samples were cooled to room temperature before application onto a nitrocellulose membrane using a 96-well vacuum manifold (Bio-Rad). For visualization of His-tagged protein content, a single-step nickel–horseradish peroxidase conjugate was used (His-probe; Pierce).

Membrane-associated expression

Twenty-milliliter cultures were grown in accordance with previously identified conditions. Cells were disrupted by sonication, and debris was removed by centrifugation at 10,000g for 5 min. Membranes were collected by ultracentrifugation at 150,000g for 20 min. The His-tagged protein content of the membrane fraction was analyzed either by dot blot or by SDS-PAGE.

For semiquantitative analysis of His-tagged protein content, micrographs were scanned using an Alpha Innotech imager. Protein bands (or dots) were quantified using the NIH Image 1.62 software.

Detergent extraction

Detergents at a final concentration of 1% were added to a 1-mg/ml membrane protein suspension. Samples were agitated for 30 min at 4 °C, and insoluble material was removed by ultracentrifugation at 100,000g for 20 min. The His-tagged protein content of the soluble fraction was analyzed either by dot blot or by SDS-PAGE.

Purification

One-liter cultures were grown in accordance with previously identified conditions. Cells (typically 3–5 g/L culture) were collected by centrifugation and disrupted using a microfluidizer processor (Microfluidics, Newton, MA) at ~18,000 psi. Prior to disruption, DNase I (Sigma) was added at 30 µg/ml to reduce the viscosity of the suspension. Unbroken cells and debris were removed by centrifugation at 8000g for 10 min, and membranes were collected by ultracentrifugation. The soluble fraction following detergent extraction was directly added to 1.5 ml of Ni-NTA superflow resin (Qiagen) or 1.5 ml of Talon resin (ClonTech). Following 16 h of gentle agitation at 4 °C, the resin was collected by brief centrifugation (2 min at 700g) and moved to disposable 10-ml columns. Contaminants were removed by washing with 20 column volumes of 20 mM Tris–HCl (pH 8), 500 mM NaCl, 5 mM β-mercaptoethanol, 20 mM imidazole, and detergent at a final concentration one to three times that of the critical micelle concentration. Additional washes with 40–100 mM imidazole were used for some proteins, and elution of the His-tagged targets was observed at 100–350 mM imidazole (protein-specific). The purity of eluted fractions was visualized by Coomassie blue staining of SDS-PAGE gels.

Gel-filtration analysis and stability assays

Purified proteins were concentrated using a 100-kDa concentrator (Amicon-Ultra; Millipore) and washed once by a 10-fold addition of buffer without imidazole. Protein concentrations were measured by absorbance at 280 nm or with Bio-Rad's RC DC Protein Assay kit. Typically, 100 µl of concentrated protein (10–20 mg/ml) was injected onto a Superdex 200 gel-filtration column (GE Healthcare). Samples were injected either at the time of preparation or following 7–10 days of storage under different conditions, as indicated.

Metal sensitivity assays

Cultures of *E. coli* W3110 or *E. coli* GG48[40] expressing the indicated proteins were diluted to an optical density (600 nm) of 0.05 in 150 µl of LB medium supplemented with 0.01% L-arabinose. Cells were grown on 96-well plates in an automated plate reader (Saffire II; Tecan Austria) with increasing amounts of $ZnCl_2$ or $CdCl_2$.

Acknowledgements

References

1. Busch, W. & Saier, M. H. J. (2002). The transporter classification (TC) system. *Crit. Rev. Biochem. Mol. Biol.* **27**, 287–337.

2. Locher, K. P., Bass, R. B. & Rees, D. C. (2003). Breaching the barrier. *Science*, **301**, 603–604.

3. Everett, L. A. & Green, E. D. (1999). A family of mammalian anion transporters and their involvement in human genetic diseases. *Hum. Mol. Genet.* **8**, 1883–1891.

4. Borst, P. & Elferink, R. O. (2002). Mammalian ABC transporters in health and disease. *Annu. Rev. Biochem.* **71**, 537–592.

5. Hilgemann, D. W., Yaradanakul, A., Wang, Y. & Fuster, D. (2006). Molecular control of cardiac sodium homeostasis in health and disease. *J. Cardiovasc. Electrophysiol.* **17**, S47–S56.

6. Camacho, A. & Massieu, L. (2006). Role of glutamate transporters in the clearance and release of glutamate during ischemia and its relation to neuronal death. *Arch. Med. Res.* **37**, 11–18.

7. MacDonald, K. D., McKenzie, K. R. & Zeitlin, P. L. (2007). Cystic fibrosis transmembrane regulator protein mutations: 'class' opportunity for novel drug innovation. *Paediatr. Drugs*, **9**, 1–10.

8. Bressler, J. P., Olivi, L., Cheong, J. H., Kim, Y., Maerten, A. & Bannon, D. (2007). Metal transporters in intestine and brain: their involvement in metal-associated neurotoxicities. *Hum. Exp. Toxicol.* **26**, 221–229.

9. Axelsen, K. B. & Palmgren, M. G. (1998). Evolution of substrate specificities in the P-type ATPase superfamily. *J. Mol. Evol.* **46**, 84–101.

10. Toyoshima, C., Nakasako, M., Nomura, H. & Ogawa, H. (2000). Crystal structure of the calcium pump of sarcoplasmic reticulum at 2.6 A resolution. *Nature*, **405**, 647–655.

11. Toyoshima, C. (2007). Ion pumping by calcium ATPase of sarcoplasmic reticulum. *Adv. Exp. Med. Biol.* **592**, 295–303.

12. Morth, J. P., Pedersen, B. P., Toustrup-Jensen, M. S., Sorensen, T. L., Petersen, J., Andersen, J. P., Vilsen, B. *et al.* (2007). Crystal structure of the sodium-potassium pump. *Nature*, **450**, 1043–1049.

13. Pedersen, B. P., Buch-Pedersen, M. J., Morth, J. P., Palmgren, M. G. & Nissen, P. (2007). Crystal structure of the plasma membrane proton pump. *Nature*, **450**, 1111–1114.

14. Arguello, J. M. (2003). Identification of ion-selectivity determinants in heavy-metal transport P_{1B}-type ATPases. *J. Membr. Biol.* **195**, 93–108.

15. Cox, D. W. & Moore, S. D. (2002). Copper transporting P-type ATPases and human disease. *J. Bioenerg. Biomembr.* **34**, 333–338.

16. Chang, G., Spencer, R. H., Lee, A. T., Barclay, M. T. & Rees, D. C. (1998). Structure of the MscL homolog from *Mycobacterium tuberculosis*: a gated mechanosensitive ion channel. *Science*, **282**, 2220–2226.

17. Kendrew, J. C. & Parrish, R. G. (1957). The crystal structure of myoglobin: III. Sperm-whale myoglobin. *Proc. Roy. Soc. London Ser. A*, **238**, 305–324.

18. Locher, K. P., Lee, A. T. & Rees, D. C. (2002). The *E. coli* BtuCD structure: a framework for ABC transporter architecture and mechanism. *Science*, **296**, 1091–1098.

19. Ames, G. F. (1968). Lipids of *Salmonella typhimurium* and *Escherichia coli*: structure and metabolism. *J. Bacteriol.* **95**, 833–843.

20. Garrity, G. M., Bell, J. A. & Lilburn, T. G. (2004). Taxonomic outline of the prokaryotes, 2nd edit. Springer-Verlag, New York, doi:10.1007/bergeysoutline200405.

21. Kashino, Y. (2003). Separation methods in the analysis of protein membrane complexes. *J. Chromatogr. B*, **797**, 191–216.

22. Mohanty, A. K. & Wiener, M. C. (2004). Membrane protein expression and production: effects of polyhistidine tag length and position. *Protein Expression Purif.* **33**, 311–325.

23. Esposito, D. & Chatterjee, D. K. (2006). Enhancement of soluble protein expression through the use of fusion tags. *Curr. Opin. Biotechnol.* **17**, 353–358.

24. Miroux, B. & Walker, J. E. (1996). Over-production of proteins in *Escherichia coli*: mutant hosts that allow synthesis of some membrane proteins and globular proteins at high levels. *J. Mol. Biol.* **260**, 289–298.

25. Drew, D. E., von Heijne, G., Nordlund, P. & de Gier, J. W. (2001). Green fluorescent protein as an indicator to monitor membrane protein overexpression in *Escherichia coli*. *FEBS Lett.* **507**, 220–224.

26. Korepanova, A., Gao, F. P., Hua, Y., Qin, H., Nakamoto, R. K. & Cross, T. A. (2005). Cloning and expression of multiple integral membrane proteins from *Mycobacterium tuberculosis* in *Escherichia coli*. *Protein Sci.* **14**, 148–158.

27. Surade, S., Klein, M., Stolt-Bergner, P. C., Muenke, C., Roy, A. & Michel, H. (2006). Comparative analysis and "expression space" coverage of the production of prokaryotic membrane proteins for structural genomics. *Protein Sci.* **15**, 2178–2189.

28. Fiermonte, G., Walker, J. E. & Palmieri, F. (1993). Abundant bacterial expression and reconstitution of an intrinsic membrane-transport protein from bovine mitochondria. *Biochem. J.* **294**, 293–299.

29. Kiefer, H., Krieger, J., Olszewski, J. D., Von Heijne, G., Prestwich, G. D. & Breer, H. (1996). Expression of an olfactory receptor in *Escherichia coli*: purification, reconstitution, and ligand binding. *Biochemistry*, **35**, 16077–16084.

30. Borths, E. L., Poolman, B., Hvorup, R. N., Locher, K. P. & Rees, D. C. (2005). In vitro functional characterization of BtuCD-F, the *Escherichia coli* ABC transporter for vitamin B12 uptake. *Biochemistry*, **44**, 16301–16309.

31. Lacapere, J. J., Robert, J. C. & Thomas-Soumarmon, A. (2000). Efficient solubilization and purification of the gastric H^+, K^+-ATPase for functional and structural studies. *Biochem. J.* **345**, 239–245.

32. Powell, L. D. & Cantley, L. C. (1980). Structural changes in $(Na^+ + K^+)$-ATPase accompanying detergent inactivation. *Biochim. Biophys. Acta*, **599**, 436–447.

33. Abramson, J., Smirnova, I., Kasho, V., Verner, G., Kaback, H. R. & Iwata, S. (2003). Structure and mechanism of the lactose permease of *Escherichia coli*. *Science*, **301**, 610–615.

34. Hunte, C., Screpanti, E., Venturi, M., Rimon, A., Padan, E. & Michel, H. (2005). Structure of a Na^+/H^+ antiporter and insights into mechanism of action and regulation by pH. *Nature*, **435**, 1197–1202.

35. Raman, P., Cherezov, V. & Caffrey, M. (2006). The Membrane Protein Data Bank. *Cell. Mol. Life Sci.* **63**, 36–51.

36. Clarke, K., Gray, G. W. & Reaveley, D. A. (1967). The cell walls of *Pseudomonas aeruginosa*. General composition. *Biochem. J.* **105**, 749–754.

37. Inamoto, Y., Ariyama, S., Hamanaka, Y., Okita, K., Kaneta, Y., Nagate, T. *et al.* (1993). Lipid analysis of *Helicobacter pylori*. *J. Clin. Gastroenterol.* **17**, S136–S139.

38. DiRusso, C. C. & Nystrom, T. (1998). The fats of *Escherichia coli* during infancy and old age: regulation by global regulators, alarmones and lipid intermediates. *Mol. Microbiol.* **27**, 1–8.

39. Hou, Z. J., Narindrasorasak, S., Bhushan, B., Sarkar, B. & Mitra, B. (2001). Functional analysis of chimeric proteins of the Wilson Cu(I)-ATPase (ATP7B) and ZntA, a Pb(II)/Zn(II)/Cd(II)-ATPase from *Escherichia coli*. *J. Biol. Chem.* **276**, 40858–40863.

40. Grass, G., Fan, B., Rosen, B. P., Franke, S., Nies, D. H. & Rensing, C. (2001). ZitB (YbgR), a member of the cation diffusion facilitator family, is an additional zinc transporter in *Escherichia coli*. *J. Bacteriol.* **183**, 4664–4667.

41. Rapp, M., Seppala, S., Granseth, E. & von Heijne, G. (2007). Emulating membrane protein evolution by rational design. *Science*, **315**, 1282–1284.

42. Bass, R. B., Strop, P., Barclay, M. & Rees, D. C. (2002). Crystal structure of *Escherichia coli* MscS, a voltage-modulated and mechanosensitive channel. *Science*, **298**, 1582–1587.

43. Sukharev, S., Akitake, B. & Anishkin, A. (2007). The bacterial mechanosensitive channel MscS: emerging principles of gating and modulation. *Curr. Top. Membr.* **58**, 235–267.

44. Eshaghi, S., Hedren, M., Nasser, M. I., Hammarberg, T., Thornell, A. & Nordlund, P. (2005). An efficient strategy for high-throughput expression screening of recombinant integral membrane proteins. *Protein Sci.* **14**, 676–683.